X-ray and optical substructuring of the DAFT/FADA survey clusters

Loïc Guennou [1] , Florence Durret [2] , Christophe Adami [1], Gastão B. Lima Neto [3]
Melville P. Ulmer [4], Douglas Clowe[5] and the DAFT/FADA collaboration

1. LAM, OAMP, Pôle de l'Etoile, Site de Château-Gombert, 38 rue F. Joliot-Curie, 13388 Marseille Cedex 13, France
2. IAP, CNRS UMR 7095 et Université Pierre et Marie Curie, 98bis Bd Arago, 75014 Paris, Franc
3. IAG, USP, Rua do Matão 1226, 05508-090 São Paulo, Brazil
4. Department of Physics and Astronomy, Northwestern University, Evanston IL 60208-2900, USA
5. Department of Physics and Astronomy, Ohio State University, 251B Clippinger Lab, Athens OH 45701, USA

The DAFT/FADA survey

This survey is based on a rich data base for 91 medium redshift ($0.4 < z < 0.9$) massive clusters (mass larger than 2 10^{14} M_{solar}) with Hubble Space Telescope imaging available.
The PIs are C. Adami, M. Ulmer and D. Clowe.
The aims of this survey are twofold:

- Build a large database of deep imaging data on these clusters to analyse the properties of clusters in this redshift range and tie the optical and X-ray substructure growth with redshift over timescales of about 2.5 Gyrs
- Obtain constraints on dark energy

We present here the morphological properties of the subsample of clusters with XMM-Newton data.

The data

We retrieved archive XMM-Newton data of sufficient quality for 30 clusters (see full list inTable 1).
We obtained deep optical imaging for most of the 91 clusters in several bands, with various telescopes, totalling about 70 nights of 4m telescope time, plus some archive data.
We retrieved all the galaxy redshifts available in NED in a 5 arcmin region around the cluster center, and have added some redshifts obtained during several observing runs with 8m telescopes.

The X-ray analysis

The XMM-Newton data were analysed in the usual way.
The X-ray images (in majority those obtained with the pn, in some cases MOS1) were then fit with an azimuthally symmetric elliptical model.
The residuals were computed as the difference between the image and the fit (see Fig. 1).

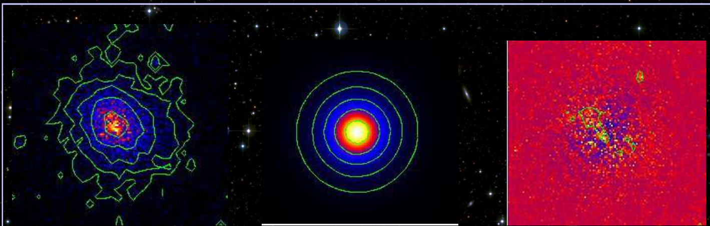

Fig. 1. XMM-Newton image (left), model (middle) and residuals (right) for Cl0016+1609.

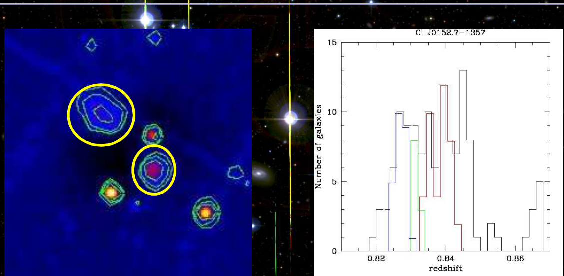

Also see Ebeling et al. 2000, ApJ 534, 133

Fig. 2. Left: residual X-ray image of the merging cluster Cl 0152.7-1357 at z=0.8310, the two components are circled in yellow, the other sources are AGN unrelated to the cluster. Right: redshift histogram for the 115 galaxies in the cluster redshift range, with the three main structures indicated in blue, green and red, colour coded as in Fig. 3, and slightly displaced to make them more visible.

Searching for optical substructures

For each cluster with more than 20 galaxy redshifts available in the cluster range, we applied the Serna & Gerbal (1996, A&A 309, 65) analysis to search for substructures. A dendogram is created, roughly representing the binding potential energy between galaxies (Fig. 3).
The number of substructures and the corresponding masses can thus be estimated (see examples for three clusters in Table 2).

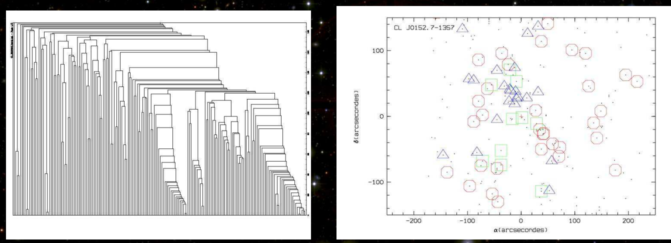

Fig. 3.Results of the Serna & Gerbal (1996) analysis for Cl 0152.7-1357 (z=0.8310). Left: dendogram showing evidence for substructures in the galaxy redshift distribution. Right: the various substructures found for this cluster plotted with different symbols (same colours as the redshift histograms in Fig. 2).

Table 1: Clusters with XMM-Newton data. The columns are: (1) name (as in NED), (2) redshift, (3) approximate number of galaxies with redshifts in the cluster range, (4) temperature of the X-ray gas, (5) X-ray luminosity in the [0.5,8] keV band.

Name	z	Nz	kT (keV)	L_X (erg s^{-1})
CL 0016+1609	0.5455	173	9.04±0.33	2.23e+45
CL J0152.7-1357	0.8310	115	6.86±0.38	7.91e+44
MS 0302.5+1717	0.4250	1	5.81±1.07	1.41e+44
RX J0337.6-2522	0.5850	5	2.45±0.57	5.73e+43
MACS J0454.1-0300	0.5377	194	9.65±0.41	2.04e+45
BMW-HRI J052215.8-362452	0.4720	1	5.13±0.50	1.70e+44
MACS J0647.7+7015	0.5907	1	8.02±0.40	1.61e+45
MACS J0744.9+3927	0.6860	2	7.58±0.25	1.87e+45
RX J0847.1+3449	0.5600	1		7.11e+44
CL 09104+4109	0.4420	2	5.33±0.14	1.58e+45
Abell 851	0.4069	213	5.16±0.15	6.13e+44
MS 1054-03	0.8231	326	9.05± 0.69	1.49e+45
UM 425 Cluster	0.7685	8	14.5±4.2	4.90e+44
MS 1137.5+6624	0.7820	17	7.31±0.77	7.41e+44
CLG J1205+4429	0.5915	10		6.77e+43
RXC J1206.2-0848	0.4400	53	9.36±0.55	2.32e+45
LCDCS 0504	0.7943	65	7.60±1.20	3.91e+44
RX J1226.9+3332	0.8900		9.00±0.39	2.02e+45
GHO 1322+3027	0.7550	38	5.25±0.99	8.91e+43
ZwCl 1332.8+5043	0.6200	1	4.71±0.55	2.40e+44
LCDCS 0829	0.4510	50	11.06±0.19	7.75e+45
LCDCS 0853	0.7627	18		3.65e+44
RX J1354.2-0221	0.5460	2		2.04e+44
GHO 1602+4312	0.8950	26	9.77±10.89	8.96e+43
MS 1621.5+2640	0.4260	104		9.13e+43
CXOU J205617.1-044155	0.6002	1	5.15±1.12	1.98e+44
MS 2053.7-0449	0.5830	30	4.73±1.03	2.13e+44
GHO 2143+0408	0.5310	1	4.86±0.47	1.51e+44
RX J2202.7-1902	0.4380	8	4.72±0.94	4.56e+43
RX J2328.8+1453	0.4970	1	2.82±0.55	4.28e+43

Table 1: Optical structures found in some clusters with X-ray data. The columns are: (1) cluster name, (2) number of the substructure, (3) number of galaxies in the substructure, (4) mean redshift of the substructure, (5) mass of the substructure.

Name		N_{gal}	z	M ($M_{\odot}$)
CL 0016+1609	1	64	0.5418	3.38e+14
	2	17	0.5505	2.04e+13
	3	13	0.5530	2.49e+13
CL J0152.7-1357	1	49	0.8376	1.23e+14
	2	17	0.8317	9.67e+12
	3	29	0.8274	9.99e+12
MACS J0454.1-0300	1	10	0.5365	1.54e+14
	2	8	0.5395	1.70e+13
	3	8	0.5307	7.72e+12
	4	6	0.5323	6.93e+12
	5	9	0.5458	8.96e+13

Results

- The studied clusters extend to z=0.9 the L_X -T_X relation established by Takey et al. (2011, A&A 534, A120) for clusters at z<0.6
- Out of 23 spatially analysed clusters, 6 have obvious substructures, 13 have possible substructures and 4 have no substructures in X-rays
- Based on comparison with simulations, there is work to be done to explain why there is apparently little X-ray luminosity evolution even though the cluster gravitational potentials are clearly evolving with time (see e.g. Ehlert & Ulmer (2009, A&A 503, 35)

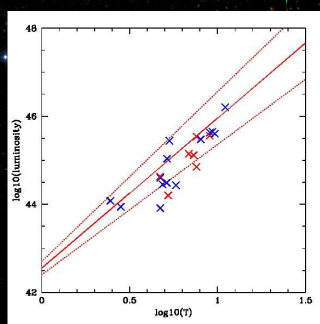

Fig. 4. L_X -T_X relation for our sample. Red crosses correspond to clusters at z>0.6 and blue crosses to z<0.6. The red line shows the Takey et al. relation for clusters at z<0.6 and the dotted lines show the 3sigma interval.

Acknowledgements. This paper is based on optical data obtained at various observatories/ telescopes: ESO, Gemini, SOAR, WYIN, WHT, TNG, Blanco, and archive data from ESO, CFHT and Subaru were also retrieved. We also acknowledge the use of the XMM-Newton and Chandra archives.